# Interference with *Prdm9*-controlled meiotic chromosome asynapsis overrides hybrid sterility in mice

Sona Gregorova[1,5], Vaclav Gergelits[1,5], Irena Chvatalova[1,2], Tanmoy Bhattacharyya[1,3], Barbora Valiskova[1,4], Vladana Fotopulosova[1], Petr Jansa[1], Diana Wiatrowska[1], Jiri Forejt[1,6]

[1]Mouse Molecular Genetics Group, Division BIOCEV, Institute of Molecular Genetics, Academy of Sciences of the Czech Republic, Průmyslová 595, 252 50 Vestec, Czech Republic.

[2]Current address: The National Institute of Public Health, Šrobárova 48, 100 42, Prague 10, Czech Republic

[3]Current address: The Jackson Laboratory, 600 Main Street | Bar Harbor, ME 04609, USA

[4]Charles University, Faculty of Science, Albertov 2038/6, 128 00, Prague 10, Czech Republic

[5]These authors contributed equally to this work

[6]To whom correspondence should be addressed: jiri.forejt@img.cas.cz

**Abstract**

The infertility of hybrids between closely related (sub)species is one of the early reproductive isolation mechanisms leading to speciation. Since the genetic control of hybrid sterility (HS) is complex, only a few HS genes have been identified so far, including *Prdm9*, the only known vertebrate HS gene. *Prdm9* causes infertility in male hybrids between PWD/Ph and C57BL/6J mouse strains derived from *Mus m. musculus* and *Mus m. domesticus* subspecies. However, within species *Prdm9* determines the sites of programmed DNA double-strand breaks (DSBs) and meiotic recombination hotspots. In sterile hybrids, different PRDM9 variants do not bind both homologous chromosomes equally, suggesting that the asymmetry or lack of symmetry of binding sites could explain the failure of meiotic chromosomes to synapse. To investigate the relation between asynapsis and meiotic arrest, we prepared intersubspecific hybrids with stretches of consubspecific homology on several pairs of autosomes and analyzed their ability to form synaptonemal complexes. Eight examined autosomes with more than 27 Mb of consubspecific homology fully restored their synapsis and we predicted that a minimum of two symmetric DSBs per chromosome are necessary for successful meiosis. Moreover, targeted suppression of asynapsis in four chromosomes most sensitive to asynapsis partially rescued spermatogenesis, thus pointing to chromosomal quality of hybrid sterility. We hypothesize that reduced ability of meiotic chromosomes to synapse, determined by impaired recombination between evolutionary diverged homologous chromosomes could function as an ancient mechanism of hybrid sterility occurring in various sexually reproducing species.

## Introduction

Hybrid sterility (HS) is a postzygotic reproductive isolation mechanism that safeguards speciation by restricting gene flow between related taxa. HS is a universal phenomenon observed in many eukaryotic inter-species hybrids, including yeast, plants, insects, birds, and mammals (1, 2). In the early days of genetics, HS had been difficult to accommodate in Darwin's theory of evolution by natural selection until the Bateson - Dobzhansky - Muller incompatibility (BDMI) hypothesis (3-5) explicated HS and, more generally, any hybrid incompatibility, as a consequence of the independent divergence of mutually interacting genes resulting in aberrant interaction of the new alleles, previously not tested by natural selection. HS has several common features across various sexually reproducing eukaryotic species. Haldane's rule posits that if one sex of the F1 offspring of two different animal races is absent, rare, or sterile, it is the heterogametic sex (XY or ZW) (6). Another common feature refers to the disproportionately large role of Chr X compared to autosomes in reproductive isolation (7). More recently, interaction between selfish genomic elements causing meiotic drive and their suppressors has been implicated in some instances of reproductive isolation (8, 9)

The molecular mechanisms underlying HS remain an unresolved question. Originally, genic and chromosomal mechanisms of HS were hypothesized, but the latter were soon dismissed as unlikely on the grounds that large chromosomal rearrangements do not segregate with HS genetic factors. Other forms of non-genic chromosomal HS were not considered because of the limited knowledge of the carrier of genetic information at the time. Thus, for the last 80 years or so, the focus on the genic control of HS prevailed (3, 5, 10). In studies mapping HS genes, the *Drosophila* group of species has been the model of choice, yet only five *Drosophila* HS genes, namely *OdsH*, *JYAlpha*, *Ovd*, *agt,* and *Taf1*, have been identified so far, none of which has a known interacting gene as predicted by the BDMI hypothesis (11-13). The low success rate of the positional cloning of HS genes was explained by the oligogenic or polygenic nature of HS phenotypes and by the inherent difficulty in genetically dissecting the phenotype that prevents its own transfer to progeny.

Over forty years ago, we introduced the house mouse (*Mus musculus*) as a mammalian model for the genetic analysis of HS. The first HS locus *Hst1* was

mapped in crosses of laboratory inbred strains (predominantly of *Mus musculus domesticus* (*Mmd*) origin) with wild *Mus musculus musculus* (*Mmm*) mice (14). Later, we developed PWD/Ph and PWK/Ph inbred strains from the wild *Mmm* mice of Central Bohemia (15) and used them in the positional cloning of *Hst1* by high-resolution genetic crosses and physical mapping (16, 17). Finally, we identified the *Hst1* locus with the PR domain containing 9 gene (*Prdm9*), coding for histone H3 lysine 4/ lysine 36 methyltransferase (18, 19), the first and still the only HS gene known in vertebrates. Most of the tested laboratory inbred strains share either the $Prdm9^{Dom2}$ or $Prdm9^{Dom3}$ allele. (20, 21). The former allele was found in inbred strains producing sterile male hybrids when crossed with PWD females, while the $Prdm9^{Dom3}$ was observed in the strains that yielded quasi-fertile males in the same type of inter-subspecific crosses (22).

The male sterility of (PWD x C57BL/6)F1 (henceforth PB6F1) hybrids depends on the interaction of the heterozygous allelic combination $Prdm9^{Msc}/Prdm9^{Dom2}$ with the PWD allelic form of the X-linked Hybrid sterility X chromosome 2 $Hstx2^{Msc}$ locus (23, 24). For the sake of clarity and to stress the origin of the alleles we will use $Prdm9^{PWD}$, $Prdm9^{B6}$ and $Hstx2^{PWD}$ in the rest of this paper. Any other tested allelic combination of these two major HS genes yields fully fertile or subfertile male hybrids (23, 25). The proper allelic combination of *Prdm9* and *Hstx2* genes is necessary but not sufficient to completely govern HS because less than 10% instead of expected 25% of (PWD x B6) x B6 male backcross progeny replicated the infertility of male PB6F1 hybrids (23). Initially, we explained this 'missing heritability' by assuming additional genic interaction of three additional HS genes with a small effect that escaped the genetic screen (23). However, an alternative, non-genic explanation emerged from the analysis of meiotic phenotypes of sterile hybrids. The failure of multiple autosomal pairs to synapse properly, the persistence of phosphorylated histone **γ**H2AX indicating unrepaired DNA double-strand breaks (DSBs) on unsynapsed chromosomes, and the disturbed transcriptional inactivation of sex chromosomes at the first meiotic prophase were the most prominent features observed in approximately 90% of primary spermatocytes of infertile PB6F1 inter-subspecific hybrids. We suggested that the failure of chromosomes to synapse could be related to their fast-evolving nongenic DNA divergence (24, 26). Because failure of proper synapsis in pachytene spermatocytes is known to interfere with the normal

progression of the first meiotic division (27, 28), the asynapsis could be the ultimate cause of the sterility of male hybrids (24, 26). Recently, the important function of PRDM9 zinc finger domain binding sites within noncoding genomic DNA has been demonstrated in male HS. Replacement of the mouse sequence encoding the PRDM9 zinc-finger array with the orthologous human sequence reversed sterility in (PWD x B6-*Prdm9*$^{Hu}$)F1 hybrid males (29). In PB6F1 hybrids, roughly 70% of *Prdm9*-directed DSBs hotspots identified by the DMC1 ChIP-seq method were asymmetric, enriched on the 'nonself' homologous chromosome, since the DSBs determined by the B6 allele of *Prdm9* were found predominantly or exclusively on PWD chromosomes, and *vice versa*. Chromosome-specific quantification of asymmetry correlated well with the asynapsis rate across five arbitrarily chosen chromosomes of PB6F1 hybrids (29, 30). Another, non-exclusive interpretation of DMC1 ChIP-seq data pointed to significant enrichment of PRDM9-independent hotspots in the PB6F1 hybrid testis, which occurs in promoters and other regulatory motifs and which is characteristic of spermatogenic arrest in *Prdm9* knockout males (30). Finally, Yamada et al. (2017) reported that one third of PRDM9-depndent DSBs occur within sequences that have at least some repetitive character and hypothesized that inappropriately high DSB levels in retroposons and other repetitive elements may contribute to the infertility seen in some mouse hybrids (31).

In this work, we experimentally verified the relationship between meiotic chromosome asynapsis, intersubspecific heterozygosity and male HS in a series of hybrids carrying recombinant chromosomes with *Mmm/Mmm* consubpecific (belonging to the same subspecies) PWD/PWD homozygous intervals on *Mmm/Mmd* heterosubpecific (belonging to different subspecies), PWD/B6 heterozygous background. We have found that targeted suppression of asynapsis in the four most asynapsis-sensitive chromosomes leads to the reversal of HS.

## Results

### Small chromosomes are more susceptible to asynapsis in sterile F1 hybrids

First, we ascertained the frequency of meiotic asynapsis for each chromosome pair of PB6F1 hybrid males by combining fluorescence in-situ hybridization (FISH) to decorate chromatin from individual chromosomes with immunostaining of the

synaptonemal complex protein 3 (SYCP3) a major component of axial/lateral elements to visualize synaptonemal complexes, and a HORMA domain-containing protein-2, HORMAD2 (32), to identify the axial elements of unsynapsed chromosomes (Fig. S1*A*). Altogether 4168 pachynemas from 40 PB6F1 hybrid males were analyzed (Table S1). All autosomes of hybrid males displayed a certain degree of asynapsis, classified as complete, partial, or intermingled, with frequencies ranging from 2.4% (Chr 1) to 42.3% (Chr 19). A strong bias was evident towards higher asynapsis rates most remarkably seen in the five smallest autosomes ($P < 5.3x10^{-14}$, comparison of GLMM models, (Fig. 1*A*). Recently, SPO11 oligos released during the processing of DSBs were sequenced, mapped and quantified at chromosome-wide scale in male mice of the B6 laboratory inbred strain (33). This information, together with the established frequency of asymmetric breaks in PBF1 hybrids (29) permits us to calculate the possible correlation between the number of symmetric DSBs per chromosome and synapsis of heterosubspecific homologs. The calculation is based on the following premises: (i) the overall densities of DSBs on individual chromosomes of B6 and PB6F1 hybrid males are similar, (ii) approximately 250 DSBs occur per leptotene/zygotene cell (34), and (iii) the 0.28 ratio of symmetric DSBs in (PWD x B6)F1 hybrid males (29) is constant in all autosomes. Under these circumstances, a strong negative correlation (Spearman's $\rho$=-0.76, P = 0.0002) of asynapsis rate with symmetric DSBs (33) can be inferred (Fig. 1B and Table S2). This correlation is stronger than the correlation of the asynapsis rate with the chromosomal length. In addition, the asynapsis rate cannot be better explained by the chromosomal length (P = 0.709, comparison of GLMM models), when it is controlled for the symmetric DSBs (SPO11 oligos), while it is better explained by the symmetric DSBs (SPO11 oligos) when controlled for chromosomal length (P = 0.046, comparison of GLMM models).

Thus our findings support the hypothesis (29, 30) that synapsis of homologous chromosomes depends on the presence of a certain minimum number of symmetric DSBs.

### Asynapsed chromosomes are devoid of active euchromatin

The Cot-1 euchromatin RNA (ecRNA) is localized throughout the active interphase chromosome territory *in cis* and does not diffuse into the rest of the nucleus like other types of RNAs. EcRNA is mainly composed of repeat-rich noncoding RNA in active,

open euchromatin (35). Accordingly, we used Cot-1 DNA as a probe for ecRNA FISH to compare the ecRNA distribution in asynapsed and synapsed chromosomes. Pachytene spermatocytes of PB6F1 hybrids were examined for subnuclear localization of active chromatin and asynapsed chromosomes using confocal fluorescence microscopy after Cot-1 RNA FISH and HORMAD2 immunolabeling. Fluorescence signal quantification revealed that subnuclear regions of asynapsed chromosomes composed of sex chromosomes and/or autosomal univalents were lacking active euchromatin in contrast to other regions of the pachytene nuclei (Fig.S1*B*, Video S1). We propose that the absence of active euchromatin is a consequence of the meiotic synapsis failure of heterosubspecific chromosomes, known as meiotic silencing of unsynapsed chromatin (MSUC (28)), which can act as a genic component contributing to the meiotic phenotypes of sterile hybrids. Our findings are in agreement with the transcriptional under-expression of genes on several autosomes and disruption of meiotic sex chromosome inactivation (MSCI) in leptotene/zygotene spermatocytes from semi-sterile *Mmm* x *Mmd* male hybrids with *Prdm9*$^{PWK/LEWES}$ and *Hstx2*$^{PWK}$ *or Hstx2*$^{LEWES}$ allelic combinations (36).

## The minimal length of consubspecific sequence necessary to rescue meiotic chromosome synapsis

We have shown previously that meiotic asynapsis affects heterosubspecific (PWD/B6) but not consubspecific (PWD/PWD) homologs in sterile male hybrids from crosses of PWD females and B6.PWD-Chr# consomic males (24, 26). Here, we searched for the minimum length of the PWD/PWD consubspecific sequence that could secure synapsis of a chromosome and potentially restore fertility in the hybrids. Instead of substituting the whole PWD chromosome for its B6 homolog, we generated recombinant PWD/B6 and B6/PWD (centromere/telomere) chromosomes. To do that, we crossed the male hybrids between two B6.PWD-Chr# consomic strains and a PWD female to match the intact maternal PWD homologs and estimated the minimum size and location of consubspecific PWD/PWD stretches needed for synapsis rescue (Fig. 2*A*).

In three 'two-chromosome crosses' (hereafter 2-chr cross) we investigated the effect of length and location of the PWD/PWD consubspecific intervals on the asynapsis rate in six different chromosomes - two in a given experiment, namely chr5 & chr12

(Tables S3, S4), chr7 & chr15 (Tables S5, S6) and chr17 & chr18 (Table S7, S8). Altogether over 12,000 pachynemas from 122 chromosomes were examined. All male progeny of the 2-chr crosses were fully sterile, with low testis weight and the absence of sperm in the epididymis. The analysis of data from six recombinant chromosomes revealed the two common features:

- Introduction by recombination of 27 Mb or more of a consubspecific (PWD/PWD) interval into a pair of intersubspecific (PWD/B6) homologs effectively suppressed the asynapsis rate below the baseline of 5 % in all six studied autosomes.

- In spite of the known role of subtelomeric (bouquet) association in chromosome pairing (37, 38), the location of the consubspecific sequence at the telomeric end was not essential for synapsis. The PWD/PWD intervals of sufficient size located at the centromeric (proximal), interstitial, or telomeric (distal) positions rescued synapsis as well (Fig. 2*B*, Tables S3-S8).

The efficiency of synapsis rescue was gradual with an apparent change point (Fig. 2B). To describe the pattern in the data a segmented regression model was used (see Materials and Methods). The model based on the data pooled from all 2-chr crosses was selected as the best model with an estimated change point estimate at 27.14 Mb (19.36; 34.91) (95% CI) (see table S9). The slope of the decrease of asynapsis in the region of consubspecific intervals shorter than 27.14 Mb was different for the respective chromosomes, reflecting the asynapsis rate in respective chromosomes in F1 cross ($P < 2 \times 10^{-16}$ F-test).

## Reversal of hybrid sterility by targeted suppression of asynapsis of four of the most asynapsis-sensitive autosomes

The above experiments have shown that a randomly located consubspecific PWD/PWD interval with a 27 or more Mb on otherwise heterosubspecific PWD/B6 background is sufficient to restore the pachytene synapsis of a given autosomal pair. To verify the causal relationship between meiotic chromosome asynapsis and HS, we attempted to reverse HS by reducing the asynapsis in the four most asynapsis-prone chromosomes. We predicted, by multiplying the probabilities of the synapsis of individual chromosomes obtained in F1 hybrids, that complete elimination of asynapsis of four of the shortest autosomes (excluding Chr 17 to avoid *Prdm9*$^{PWD/PWD}$

interference) could increase the proportion of primary spermatocytes with the full set of synapsed autosomes up to 26.7 and potentially abolish apoptosis of these cells to yield around 5 million sperm cells in the epididymis of the hybrid males.

To test the above prediction experimentally, we transferred random intervals of consomic Chrs $15^{PWD}$, $16^{PWD}$, $18^{PWD}$, and $19^{PWD}$ on the genetic background of B6 mice in a three-generation cross (Fig. 3*A*). Eleven G3 males selected for maximal extent of PWD sequence on these chromosomes were crossed to PWD females (Table S10). The resulting G4 hybrid male progeny (hereafter 4-chr cross) displayed various degrees of PWD homozygosity in the studied consomic autosomes on otherwise heterosubspecific PWD/B6 genetic background. As predicted, a significant fraction of hybrid males showed partial rescue of spermatogenesis. While in the PB6F1 cross, 100 % of hybrid males showed no sperm in the epididymis, in the 4-chr cross, only 51.7 % of 87 G4 males were aspermic, 19.5 % had a 0.01–0.74 x $10^6$ sperm count, and 28.7 % had 1.0–13.7 x $10^6$ sperm cells (Fig. S2, Table S11).

Next, we asked whether the reversal of meiotic arrest correlates with the recovery of meiotic synapsis of recombined chromosomes and with the size of PWD/PWD consubspecific stretches in the four manipulated chromosomes. Eighteen G4 males were deliberately selected according to their fertility parameters, 13 with HS partial rescue, displaying sperm cells in the epididymis (0,1 x 10–6,9 x $10^6$), and five aspermic controls. The meiotic analysis of over 6500 pachynemas from the genotyped males indeed confirmed the prediction based on the results of 2-chr crosses. The nonrecombinant PWD/PWD consubspecific bivalents were always fully synapsed, while all nonrecombinant PWD/B6 heterosubspecific pairs revealed the highest frequencies of asynapsis. All recombinant chromosomes with consubspecific intervals of sufficient length (Fig. 3*B*, Table S12; see Table S9 for change point estimates) effectively restored synapsis. Moreover, the presence of sperm cells corresponded with the rescue of synapsis of consomic chromosomes. As a rule of thumb, the hybrids had sperm when asynapsis was suppressed in at least three of four segregating chromosomes and when the probability of all four consomic chromosomes being synapsed was > 0.7 (Fig. 3*C*). Chromosomes 16, 18, and 19 contributed the strongest effect (Table S12).

## Evidence for a trans-effect on the rate of asynapsis

Provided the probability of failure of the synapsis of each chromosome was completely independent of the rest of the hybrid genome, the asynapsis rate of the nonrecombinant heterosubspecific chromosomes would be the same in F1 hybrids, 2-chr crosses, and 4-chr cross. Moreover, the frequency of pachynemas with all chromosomes synapsed could be predicted from the observed frequencies of the synapsis of individual chromosomes. Such predicted values would be close to the values directly read from the meiotic spreads and would lie along the diagonal in Fig. 4. As shown below, both types of analysis clearly revealed that the asynapsis rate of a particular chromosome depends on the synapsis status of other chromosomes.

In PB6F1 hybrids, the observed 13.1 % (11.4 %, 14.9 %) (95 % CI) of fully synapsed pachynemas was double (P = 0.023, Mann-Whitney test) the rate expected by the multiplication of the observed synapsis rates 6.6 % (5.3 %, 8.1 %) of individual chromosomes (Fig. 4), indicating a stochastic *trans* effect of synapsed autosomes on the probability of the asynapsis of other heterosubspecific chromosome pairs. The tendency is more pronounced in data from 2-chr crosses and 4-chr cross experiments. The most straightforward comparison is between the nonrecombinant PWD/B6 heterosubspecific chromosomes from F1 hybrids and 2-chr cross or 4-chr crosses, where the asynapsis rate is dramatically reduced to 58–91 % of the respective F1 hybrids' rates. Moreover, the difference between the observed and expected ratios of asynaptic pachynemas increased with increasing probability of sperm cells in the epididymis (Fig. 4, Table S13). In 4-chr cross, the *trans* effect was analyzed further by comparing the asynapsis rate of a given nonrecombinant PWD/B6 pair with the other three analyzed chromosomes. Figure S4 shows a negative correlation (from r= -0.45 for Chr 16 to r = -0.88 for Chr 15, linear regression slope is $\beta_{3_chrs_syn}$ = -0.19, P = 0.0003) between the asynapsis rate of the nonrecombinant chromosome and the probability of synapsis of the other three studied chromosomes.

To conclude, the described *trans* effect enhances the probability of the successful pairing of heterosubspecific chromosomes in males with identical *Prdm9* and *Hstx2*. The mechanism is unknown, but it is tempting to speculate that a rate-limiting step of an anti-recombination mismatch repair machinery (39, 40) could be involved.

## Discussion

While the genic control of HS and meiotic synapsis in PBF1 hybrids can be demonstrated by complete restitution of fertility and meiotic pairing in males with *Prdm9*$^{PWD/PWD}$ or *Prdm9*$^{PWD/B6Hu}$ genotypes and partial recovery in *Prdm9*$^{PWD/C3H}$ males (23, 26, 29), a chromosome-autonomous nature of asynapsis became apparent in experiments where PB6F1 hybrids carried a single pair of PWD/PWD consubspecific homologs. The males remained sterile, but synapsis of the particular consubspecific pair was completely restored (26). Such regulation of meiotic asynapsis in PBF1 hybrids can be explained by a combined effect of the chromosome-autonomous interaction of homologs operating *in cis* and *Prdm9/Hstx2* incompatibility operating *in trans*. Here we separated the non-genic from genic control mechanisms by keeping the sterility-determining allelic combination of the *Prdm9*$^{PWD}$/*Prdm9*$^{B6}$ gene and *Hstx2*$^{PWD}$ locus constant in all crosses, while successively introgressing stretches of the PWD/PWDconsubspecific sequence into eight PWD/B6 heterosubspecific autosomal pairs.

### The meiotic asynapsis rate correlates with the presumed paucity of symmetric DSBs in individual chromosomes in sterile hybrids

The first direct evidence on the molecular mechanism of *Prdm9*'s control of meiotic arrest in sterile hybrids came from the 'humanized' mouse *Prdm9*$^{B6Hu}$ allele created by substituting the mouse PRDM9 zinc finger array with its human counterpart. Davies and coworkers (29) proved that the DNA-binding zinc finger domain of PRDM9 molecule is responsible for sterility in PB6F1 hybrids. In the sterile hybrids, most PRDM9$^{PWD}$-specific hotspots reside on B6 chromosomes and, *vice versa*, most of the PRDM9$^{B6}$ binding sites are activated on PWD chromosomes. This asymmetry was explained in part by erosion of the PRDM9 binding sites due to preferential transmission to progeny of the mutated hotspots motifs (41, 42). The authors proposed that asymmetry of the *Prdm9*-dependent DSB hotspots and the consequent shortage of symmetric hotspots is the major culprits of meiotic asynapsis and meiotic arrest. In a parallel study, Smagulova and coworkers (30) used a panel of mouse inbred strains from four major *Mus musculus* subspecies to study recombination-initiating hotspots. In PB6F1 hybrids, a novel class of strong hotspots absent in both parents appeared, 70 % of them showing the asymmetry also

described in (29). Moreover, *Prdm9*-independent 'default' hotspots were particularly enriched in Chr X and percentage of ‘default’ hotspots in autosomes (26) correlate with the present data on asynapsis rate in F1 hybrids (Spearman’s $\rho$ = 0.69, P = 0.0012). These hotspots could represent the late-forming DSBs on unsynapsed chromosomes and, as such, they may be a consequence rather than the cause of meiotic asynapsis.

We show that meiotic asynapsis affects each autosomal pair in PB6F1 intersubspecific hybrids at distinctively unequal rates, with shorter chromosomes affected more often than the longer ones. A similar pattern of higher sensitivity of smaller autosomes to the synapsis failure was observed in mice with lowered dosages of SPO11 (34) and consequent twofold DSB reduction. The fact that the asynapsis rate of sterile F1 hybrids correlates better with SPO11-oligo derived density (inferred from B6 mouse strain data (33) than with the chromosome length further supports the idea (29) that the asynapsis in sterile PB6F1 hybrids is caused by an insufficient number of symmetric DSBs.

## Small stretches of consubspecific sequence restore the synapsis of heterosubspecific chromosomes

Provided that a shortage of symmetric DSB hotspots (29) is the ultimate cause of failure of meiotic synapsis of heterosubspecific homologs, then by exchanging the asymmetric hotspots for the symmetric ones the full synapsis could be restored. To experimentally test this assumption, we constructed pairs of PWD/B6 heterosubspecific homologs with stretches of PWD/PWD consubspecific intervals, which by definition cannot carry asymmetric hotspots. We found that chromosomes with 27 Mb or longer stretches of consubspecific PWD/PWD sequence always rescued full synapsis in hybrid males between PWD females and consomic B6.PWD-Chr # males. The position of the consubspecific interval along the chromosome was not critical for synapsis rescue, in accordance with the finding that synaptonemal complexes nucleate at multiple recombination sites in each chromosome (43, 44). We hypothesize that the presence of symmetric DSBs hotspots within the PWD/PWD homozygous stretches exceeded the threshold of a minimum number of symmetric DSBs thus rescuing normal meiotic synapsis.

A tentative estimate of the number of DSBs necessary for proper synapsis was based on several assumptions, namely that the number of DSBs per early zygonema is 250 DSBs ± 20 (SD) (26, 34, 45), that the DSBs are distributed across the chromosomes in proportion to the SPO11 oligos released by individual chromosomes (33) and that the sterile F1 hybrids display only 28 % of symmetric DSBs (29, 30) randomly distributed on individual autosomes. The presumed distribution of symmetric DSBs on all autosomes and their asynapsis ratios in sterile F1 hybrids are given in Table S2. Based on the above-mentioned assumptions and measured asynapsis rate in this study and in our previous work (26), we aimed to model how the induction and repair of DSBs influence proper meiotic synapsis, and tried to estimate the minimum number of symmetric DSBs per chromosome sufficient for full meiotic synapsis. Our model predicts that in approximately 25 % of cases, a chromosome is asynapsed because there is no symmetric DSB (median of P(asynapsis) / P(0 symmetric DSBs) = 4.52). Assuming a critical threshold of the required DSBs, the remaining 75 % of asynapsis could occur on chromosomes with one symmetric DSB. It is consistent with our data that all asynapsis occurs when there is 0 or 1 symmetric DSBs (median of P(asynapsis) / P(0 or symmetric DSBs) = 1) and that two symmetric DSBs per chromosome could be sufficient for full development of the synaptonemal complex, as shown in Fig. 5 for PB6F1 hybrids. The same conclusion also holds true for 2-chr cross and 4-chr cross experiments (Fig. S4 and Fig. S5). The deviations from the diagonal in the Fig. S5 depicting 4-chr cross can be explained by the *trans*-effect described in the Results section.

## On the chromosomal nature of hybrid sterility

It has been tacitly assumed, that the early meiotic arrest in sterile PBF1 males is due to the high incidence of asynapsed chromosomes in zygotene/pachytene spermatocytes of PBF1 hybrid males (24, 26). Here we provided the first experimental validation of this assumption by targeted suppression of asynapsis rate in selected autosomes. The suppression of asynapsis in any of three combinations of two PWD/B6 recombinant chromosomes did not improve the spermatogenic arrest. However, when hybrid genomes with four short recombinant chromosomes (that are most sensitive to asynapsis) were constructed, almost 50 % of males had sperm in the epididymis and normal testis size. By improving synapsis in three of the four manipulated chromosomes (representing ~11 % of the genome) with PWD/PWD

homozygous intervals, more than 40 % of pachynemas regained full chromosome synapsis and yielded sperm. These results show that the high incidence of primary spermatocytes with asynaptic chromosomes is indeed the factor determining the extent of meiotic arrest in intersubspecific PBF1 hybrids.

The unique character of PBF1 HS lies in its chromosomal character controlled by the *Prdm9* gene. The interhomolog incompatibility caused by single nucleotide variation in PRDM9 binding sites, which are situated away from coding genes (46) is proposed to make the asymmetric sites difficult to repair (29, 47). We hypothesize that building the meiotic barrier between (sub)species begins with genome-wide accumulation of single nucleotide variants within PRDM9 binding sites and their subsequent erosion due to gene conversion-guided meiotic drive (48). In the subspecific hybrids the asymmetric binding sites can be more difficult to repair using the homolog from another subspecies as a template because of the sequence heterogeneity control by the mismatch repair machinery. Originally, such an inter-species barrier was proposed by Radman and colleagues (49, 50) to prevent homeologous recombination between *E. coli* and *Salmonella typhiimurium*. Among eukaryotes, the role of the mismatch repair system in reproductive isolation was reported in *Saccharomyces* species (51-53). An exciting possibility arises that the heteroduplex rejection activity of MMR preventing repair of DSBs due to genetic heterology (36, 37) could operate as a universal mechanism gradually restricting gene flow between related (sub)species, a *conditio sine qua non* of speciation.

## Materials and Methods

**Mice, Ethics Statement and Genotyping.** The mice were maintained at the Institute of Molecular Genetics in Prague and Vestec, Czech Republic. The project was approved by the Animal Care and use Committee of the Institute of Molecular Genetics AS CR, protocol No 141/2012. The principles of laboratory animal care, Czech Act No. 246/1992 Sb., compatible with EU Council Directive 86/609/EEC and Apendix of the Council of Europe Convention ETS, were observed. SSLP markers used for genotyping consomic chromosomes in 2-chr crosses and 4-chr cross are listed in Table S15. Detailed descriptions of inbred mouse strains, fertility testing and genotyping are given in the *SI Materials and Methods.*

**Antibodies for the immunostaining of spread spermatocytes.** Detailed descriptions of the preparation of meiotic spreads and the visualization of SYCP3, γH2AFX, and HORMAD2 proteins on spreads of meiotic cells are given in the *SI Materials and Methods.*

**DNA and RNA FISH.** To identify individual chromosomes, XMP Xcyting Mouse Chromosome N Whole Painting Probes (Metasystem) were used for DNA FISH. Identification of nascent RNA in pachytene spermatocytes was performed as previously described (54), with modifications. A detailed description is given in the *SI Materials and Methods.*

**Microscopy and image capture**. Images were observed using a Nikon Eclipse 400 epifluorescence microscope and captured with a DS-QiMc mono-chrome camera (Nikon). Images were analyzed using the NIS elements program. A detailed description is given in the *SI Materials and Methods.*

**Statistics**

All calculations were performed in the statistical environment R 3.2.2. For modeling the dependence between the asynapsis rate and the number of symmetric DSBs, we determined the probabilistic distribution of the number of symmetric DSBs. The distribution was determined by simulation and with parameters based on previous studies: (i) the number of DSBs per cell (26) was modeled as an observation from the normal distribution N (250, sd = 20). (ii) We assumed a number of DSBs proportional to Spo11 oligos (33) in each autosome. (iii) The positions of DSBs in the particular autosome were simulated from the uniform distribution, U (0, Autosome_length). (iv) For the heterosubspecific part of the autosome, the number of symmetric DSBs was simulated from the binomial distribution Bi (n = N_DSBs_in_het_part, p = 0.28) (29, 30). For the consubspecific part of the autosome, all DSBs were taken as symmetric. The total number of symmetric DSBs in the autosome was taken as the sum of symmetric DSBs in the respective parts.
Steps (i) - (iv) were performed in N = 100000 simulations to obtain a probabilistic distribution. Further details on statistical evaluation are given in the *SI Materials and Methods.*

## Acknowledgements

We thank Simon Myers for sharing his unpublished data and critical comments, Attila Tóth for providing the HORMAD2 antibody, Mary Ann Handel and Linda Odenthal-Hesse for critical reading of this manuscript, David Green, Sarka Takacova, and members of the Forejt lab for their helpful comments, M. Capek for help with analysis of confocal microscopy data, and J. Perlova for her assistance with genotyping. This work was supported by Czech Science Foundation grant 13-08078S and by the LQ1604 project of the NSPII from the Ministry of Education, Youth and Sports of the Czech Republic. Barbora Valiskova was partly supported by project GA UK No.17115 from Charles University, Czech Republic. We also acknowledge the Light Microscopy Core Facility, IMG ASCR, Prague, supported by MEYS (LM2015062), OPPK (CZ.2.16/3.1.00/21547) and (LO1419).

---

1. Coyne JA & Orr HA (2004) *Speciation* (Sinauer Associates, Sunderland, Massachusetts) p 545.
2. Maheshwari S & Barbash DA (2010) The Genetics of Hybrid Incompatibilities. *Annu Rev Genet*.
3. Dobzhansky T (1951) *Genetics and the origin of Species*, (Columbia University, New York).
4. Muller H & Pontecorvo G (1942) Recessive genes causing interspecific sterility and other disharmonies between Drosophila melanogaster and simulans. *Genetics* 27:157.
5. Orr HA (1996) Dobzhansky, Bateson, and the genetics of speciation. *Genetics* 144(4):1331-1335.
6. Haldane J (1922) Sex ration and unisexual sterility in animal hybrids. *J. Genet.* 12:101-109.
7. Presgraves DC (2008) Sex chromosomes and speciation in Drosophila. *Trends Genet* 24(7):336-343.
8. Orr HA (2005) The genetic basis of reproductive isolation: insights from Drosophila. *Proceedings of the National Academy of Sciences of the United States of America* 102 Suppl 1:6522-6526.
9. Zhang L, Sun T, Woldesellassie F, Xiao H, & Tao Y (2015) Sex ratio meiotic drive as a plausible evolutionary mechanism for hybrid male sterility. *PLoS genetics* 11(3):e1005073.
10. Forsdyke DR (2017) Speciation: Goldschmidt's chromosomal heresy, once supported by Gould and Dawkins, is again reinstated. *Biol. Theory* 12:4-12.
11. Ting C, Tsaur S, Wu M, & Wu C (1998) A rapidly evolving homeobox at the site of a hybrid sterility gene [see comments]. *Science* 282(5393):1501-1504.

12. Masly JP, Jones CD, Noor MA, Locke J, & Orr HA (2006) Gene transposition as a cause of hybrid sterility in Drosophila. *Science* 313(5792):1448-1450.
13. Phadnis N & Orr HA (2009) A single gene causes both male sterility and segregation distortion in Drosophila hybrids. *Science* 323(5912):376-379.
14. Forejt J & Ivanyi P (1974) Genetic studies on male sterility of hybrids between laboratory and wild mice (Mus musculus L.). *Genet Res* 24(2):189-206.
15. Gregorova S & Forejt J (2000) PWD/Ph and PWK/Ph inbred mouse strains of Mus m. musculus subspecies--a valuable resource of phenotypic variations and genomic polymorphisms. *Folia Biol (Praha)* 46(1):31-41.
16. Gregorova S*, et al.* (1996) Sub-milliMorgan map of the proximal part of mouse Chromosome 17 including the hybrid sterility 1 gene. *Mammalian genome : official journal of the International Mammalian Genome Society* 7(2):107-113.
17. Trachtulec Z*, et al.* (1997) Isolation of candidate hybrid sterility 1 genes by cDNA selection in a 1.1 megabase pair region on mouse chromosome 17. *Mammalian genome : official journal of the International Mammalian Genome Society* 8(5):312-316.
18. Mihola O, Trachtulec Z, Vlcek C, Schimenti JC, & Forejt J (2009) A mouse speciation gene encodes a meiotic histone H3 methyltransferase. *Science* 323(5912):373-375.
19. Powers NR*, et al.* (2016) The Meiotic Recombination Activator PRDM9 Trimethylates Both H3K36 and H3K4 at Recombination Hotspots In Vivo. *PLoS genetics* 12(6):e1006146.
20. Parvanov ED, Petkov PM, & Paigen K (2010) Prdm9 controls activation of mammalian recombination hotspots. *Science* 327(5967):835.
21. Brunschwig H*, et al.* (2012) Fine-scale maps of recombination rates and hotspots in the mouse genome. *Genetics* 191(3):757-764.
22. Forejt J, Pialek J, & Trachtulec Z (2012) Hybrid male sterility genes in the mouse subspecific crosses. *Evolution of the House Mouse*, eds Macholan M, Baird SJE, Muclinger P, & Pialek J (Cambridge University Press, Cambridge).
23. Dzur-Gejdosova M, Simecek P, Gregorova S, Bhattacharyya T, & Forejt J (2012) Dissecting the genetic architecture of f(1) hybrid sterility in house mice. *Evolution; international journal of organic evolution* 66(11):3321-3335.
24. Bhattacharyya T*, et al.* (2014) X chromosome control of meiotic chromosome synapsis in mouse inter-subspecific hybrids. *PLoS genetics* 10(2):e1004088.
25. Flachs P*, et al.* (2012) Interallelic and intergenic incompatibilities of the Prdm9 (Hst1) gene in mouse hybrid sterility. *PLoS genetics* 8(11):e1003044.
26. Bhattacharyya T*, et al.* (2013) Mechanistic basis of infertility of mouse intersubspecific hybrids. *Proceedings of the National Academy of Sciences of the United States of America* 110(6):E468-477.
27. Mahadevaiah SK*, et al.* (2008) Extensive meiotic asynapsis in mice antagonises meiotic silencing of unsynapsed chromatin and consequently disrupts meiotic sex chromosome inactivation. *J Cell Biol* 182(2):263-276.
28. Burgoyne PS, Mahadevaiah SK, & Turner JM (2009) The consequences of asynapsis for mammalian meiosis. *Nature reviews. Genetics* 10(3):207-216.
29. Davies B*, et al.* (2016) Re-engineering the zinc fingers of PRDM9 reverses hybrid sterility in mice. *Nature* 530(7589):171-+.
30. Smagulova F, Brick K, Pu YM, Camerini-Otero RD, & Petukhova GV (2016) The evolutionary turnover of recombination hot spots contributes to speciation in mice (vol 30, pg 266, 2016). *Genes & development* 30(7):871-871.

31. Yamada S*, et al.* (2017) Genomic and chromatin features shaping meiotic double-strand break formation and repair in mice. *Cell Cycle*:1-15.
32. Wojtasz L*, et al.* (2012) Meiotic DNA double-strand breaks and chromosome asynapsis in mice are monitored by distinct HORMAD2-independent and -dependent mechanisms. *Genes & development* 26(9):958-973.
33. Lange J*, et al.* (2016) The Landscape of Mouse Meiotic Double-Strand Break Formation, Processing, and Repair. *Cell* 167(3):695-708 e616.
34. Kauppi L*, et al.* (2013) Numerical constraints and feedback control of double-strand breaks in mouse meiosis. *Genes & development* 27(8):873-886.
35. Hall LL*, et al.* (2014) Stable C0T-1 repeat RNA is abundant and is associated with euchromatic interphase chromosomes. *Cell* 156(5):907-919.
36. Larson EL, Keeble S, Vanderpool D, Dean MD, & Good JM (2016) The composite regulatory basis of the large X-effect in mouse speciation. *Mol Biol Evol*.
37. Ishiguro K*, et al.* (2014) Meiosis-specific cohesin mediates homolog recognition in mouse spermatocytes. *Genes & development* 28(6):594-607.
38. Scherthan H, Schofisch K, Dell T, & Illner D (2014) Contrasting behavior of heterochromatic and euchromatic chromosome portions and pericentric genome separation in pre-bouquet spermatocytes of hybrid mice. *Chromosoma* 123(6):609-624.
39. Spies M & Fishel R (2015) Mismatch repair during homologous and homeologous recombination. *Cold Spring Harbor perspectives in biology* 7(3):a022657.
40. Chakraborty U & Alani E (2016) Understanding how mismatch repair proteins participate in the repair/anti-recombination decision. *FEMS yeast research* 16(6).
41. Myers S*, et al.* (2010) Drive against hotspot motifs in primates implicates the PRDM9 gene in meiotic recombination. *Science* 327(5967):876-879.
42. Boulton A, Myers RS, & Redfield RJ (1997) The hotspot conversion paradox and the evolution of meiotic recombination. *Proceedings of the National Academy of Sciences of the United States of America* 94(15):8058-8063.
43. Zickler D & Kleckner N (2015) Recombination, Pairing, and Synapsis of Homologs during Meiosis. *Cold Spring Harbor perspectives in biology* 7(6).
44. Finsterbusch F*, et al.* (2016) Alignment of Homologous Chromosomes and Effective Repair of Programmed DNA Double-Strand Breaks during Mouse Meiosis Require the Minichromosome Maintenance Domain Containing 2 (MCMDC2) Protein. *PLoS genetics* 12(10):e1006393.
45. Cole F*, et al.* (2012) Homeostatic control of recombination is implemented progressively in mouse meiosis. *Nat Cell Biol* 14(4):424-430.
46. Baudat F, Imai Y, & de Massy B (2013) Meiotic recombination in mammals: localization and regulation. *Nature reviews. Genetics* 14(11):794-806.
47. Auwerx J*, et al.* (2004) The European dimension for the mouse genome mutagenesis program. *Nature genetics* 36(9):925-927.
48. Baker CL*, et al.* (2015) PRDM9 drives evolutionary erosion of hotspots in Mus musculus through haplotype-specific initiation of meiotic recombination. *PLoS genetics* 11(1):e1004916.
49. Rayssiguier C, Thaler DS, & Radman M (1989) The barrier to recombination between Escherichia coli and Salmonella typhimurium is disrupted in mismatch-repair mutants. *Nature* 342(6248):396-401.

50. Stambuk S & Radman M (1998) Mechanism and control of interspecies recombination in Escherichia coli. I. Mismatch repair, methylation, recombination and replication functions. *Genetics* 150(2):533-542.
51. Hunter N, Chambers S, Louis E, & Borts R (1996) The mismatch repair system contributes to meiotic sterility in an interspecific yeast hybrid. *EMBO J* 15(7):1726-1733.
52. Liti G, Barton DBH, & Louis EJ (2006) Sequence diversity, reproductive isolation and species concepts in Saccharomyces. *Genetics* 174(2):839-850.
53. Greig D, Travisano M, Louis EJ, & Borts RH (2003) A role for the mismatch repair system during incipient speciation in Saccharomyces. *J Evol Biol* 16(3):429-437.
54. Mahadevaiah SK, Costa Y, & Turner JM (2009) Using RNA FISH to study gene expression during mammalian meiosis. *Methods Mol Biol* 558:433-444.

**Legends to figures**

**Fig. 1.** The asynapsis rate of individual autosomes in sterile male (PWD x B6)F1 hybrids. (*A*) Mean asynapsis rate ± S.E (based on GLMM model). Intermingled asynapsis refers to overlaps of two or more asynapsed chromosomes within the DNA FISH cloud of chromatin. Smaller chromosomes had higher asynapsis rate (GLMM model, $P < 1.1x10^{-13}$). Concurrently, the chromosomes with higher asynapsis rate were also more involved in complete rather than partial asynapsis (GLMM model, $P < 6.3x10^{-5}$). The proportion of complete and partial asynapsis was controlled by the asynapsis rate rather than the chromosomal length (test for effect of the length when controlled for the asynapsis rate, 0.491). (*B*) Negative correlation (Spearman's $\rho = -0.76$, $P = 0.0002$) between asynapsis rate and mean expected number of symmetric DSBs (29) based on the chromosome-wise distribution of SPO11 oligos in fertile B6 males (30) (see also Table S2).

**Fig. 2.** The effect of consubspecific PWD/PWD stretches of genomic sequence on pachytene synapsis, 2-chr cross. (*A*) The F1 hybrid males of two consomic strains (generation 1 - G1, Chr 5 and Chr 12 shown here) were crossed to PWD females to produce generation 2 - G2 sterile F1 hybrids with random recombinant consomic chromosomes 5 and 12. (*B*) Combinations of two chromosomes (5+12, 7+15 and 17+18) were challenged in each experiment. The localization of the PWD homozygous sequence with respect to the centromere, interstitial part of the chromosome, telomere, or both ends is distinguished by colors (see also Tables S3 - S8). The average length between the minimum and maximum of the conspecific sequence is plotted. The mean asynapsis rate of a given chromosome is regularly higher in PB6F1 hybrids (dashed line) than in 2-chr cross. For explanation, see Fig. 4 and the chapter on the trans-effect dependent variation in asynapsis rate. Loess curve with 95% CI.

**Fig. 3.** The effect of consubspecific PWD/PWD stretches of genomic sequence on pachytene synapsis and meiotic progression, 4-chr cross. (*A*) Scheme of a four-generation cross resulting in F1 hybrids with four recombinant consomic chromosomes. (*B*) The asynapsis rate related to the size and chromosomal position of the consubspecific PWD/PWD sequence in four consomic chromosomes (15, 16, 18, and 19, see also Table 1). The localization of the PWD homozygous sequence with respect to the centromere, interstitial part of the chromosome, telomere, or both ends is distinguished by colors (see also Tables 1). (*C*) The number of sperm in the epididymis is a function of probability of synapsis of all four consomic chromosomes. The complete meiotic arrest is reversed in males having 70% or higher chance of all four chromosomes synapsed. See also Table S11. Loess curve with 95% CI.

**Fig. 4.** The trans-acting effect of consubspecific PWD/PWD stretches increases the probability of full synapsis of PWD/B6 heterosubspecific homologs in male 2-chr cross and 4-chr cross experiments. The expected rate of synapsed pachynemas was calculated for each mouse in 2-chr cross and 4-chr cross experiments by multiplication of the observed synapsis rates (i.e., assuming independence) of FISH analyzed chromosomes and the observed PB6F1 synapsis rates of the remaining autosomes. Asynapsis rate was calculated as a complement to synapsis rate. The difference between the expected and observed overall asynapsis is most pronounced in 4-chr cross males with the lowest expected overall asynapsis rate. Recovery of spermatogenesis signaled by the presence of sperm in the epididymis occurs when more than 40 % of pachynemas are fully synapsed. SC means sperm count.

**Fig. 5.** Two or more symmetric DSBs can be sufficient for synapsis. The probabilistic distribution of symmetric DSBs is calculated based on the model described in the Discussion.

.

**Fig. S1.** Asynapsis of heterosubspecific homologs in PB6F1 pachynemas. (A) Partial (arrowheads) and complete (arrows) asynapsis of Chr 19, 11, and 13. HORMAD2-labeled chromosomes with synapsis defects often form tangles via nonhomologous pairing. (B) Asynapsed chromosomes are embedded in transcriptionally silenced chromatin visualized by the lack of ecRNA detected by Cot1 RNA FISH. See also video 1.

**Fig. S2.** Fertility parameters of G4 males from the 4-chr cross. Rescue of HS meiotic arrest is detectable in males with the weight of paired testes >70 mg and >0.1 x $10^6$ of sperm in the epididymis. The males selected for DNA FISH/HORMAD2 analysis of asynapsis are highlighted in turquoise. All males share the sterility-determining allelic combination of *Prdm9*$^{PWD/B6}$ and *Hstx2*$^{PWD}$. Loess curve with 95% CI.

**Fig. S3.** Asynapsis rate of individual nonrecombinant consomic PWD/B6 chromosomes modified in trans by the probability of synapsis of the remaining three consomic chromosomes in 4-chr cross in individual males compared to PB6F1 hybrids. Asynapsis rate of a given chromosome is in negative correlation (r = -0.88, -0.45, -0.80, -0.67 for Chrs 15, 16, 18, 19 respectively) with the probability that all other three analyzed chromosomes are synapsed. The slope of linear regressioon is $\beta_{3_chrs_syn}$ = -0.19, overall P = 0.0003.

**Fig. S4.** Two and more symmetric DSBs can be sufficient for synapsis in 2-chr cross males. See Fig. 5 for details

**Fig. S5.** Two or more symmetric DSBs can be sufficient for synapsis in 4-chr cross hybrid males. See Fig. 5 for details.

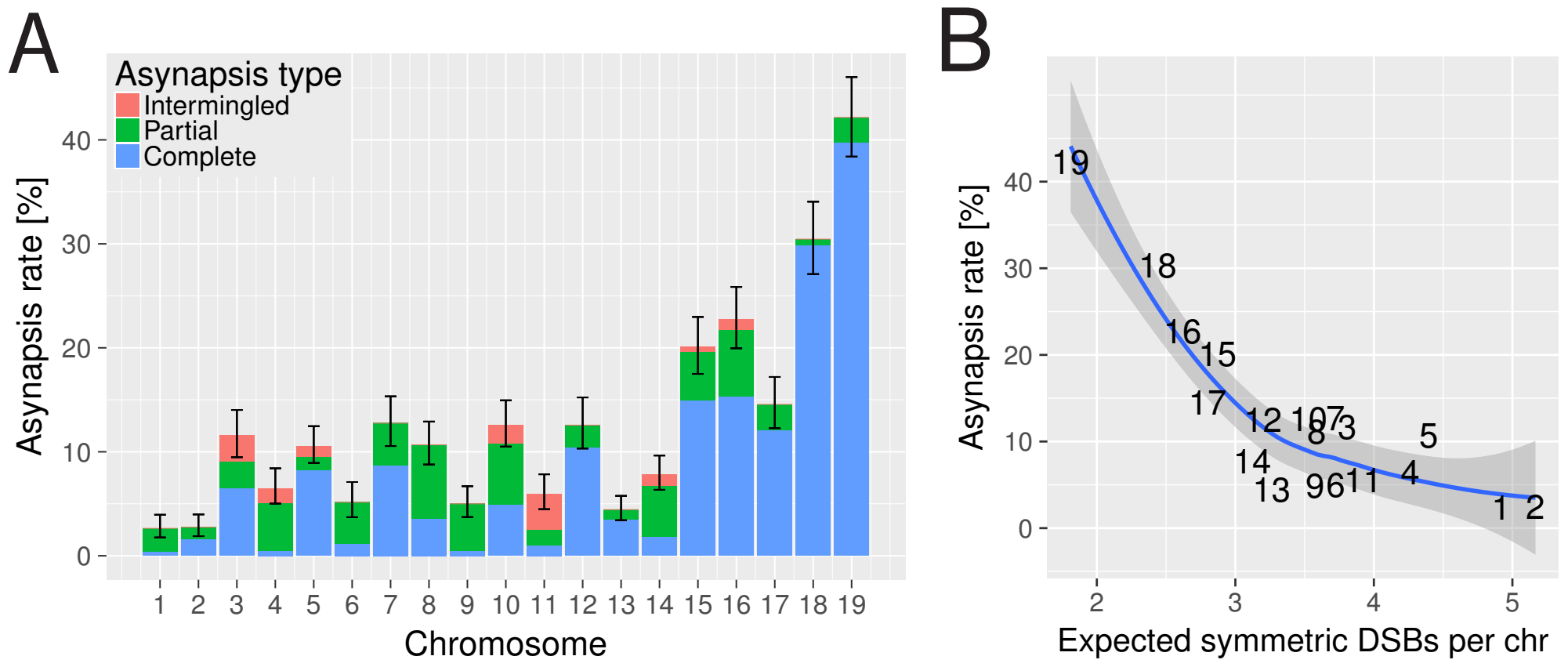
A
Asynapsis type
Intermingled
Partial
Complete
Asynapsis rate [%]
0
10
20
30
40
1 2 3 4 5 6 7 8 9 10 11 12 13 14 15 16 17 18 19
Chromosome
B
Asynapsis rate [%]
0
10
20
30
40
19
18
16
15
17
12
10
7
8
3
5
14
13
9
6
11
4
1
2
2
3
4
5
Expected symmetric DSBs per chr

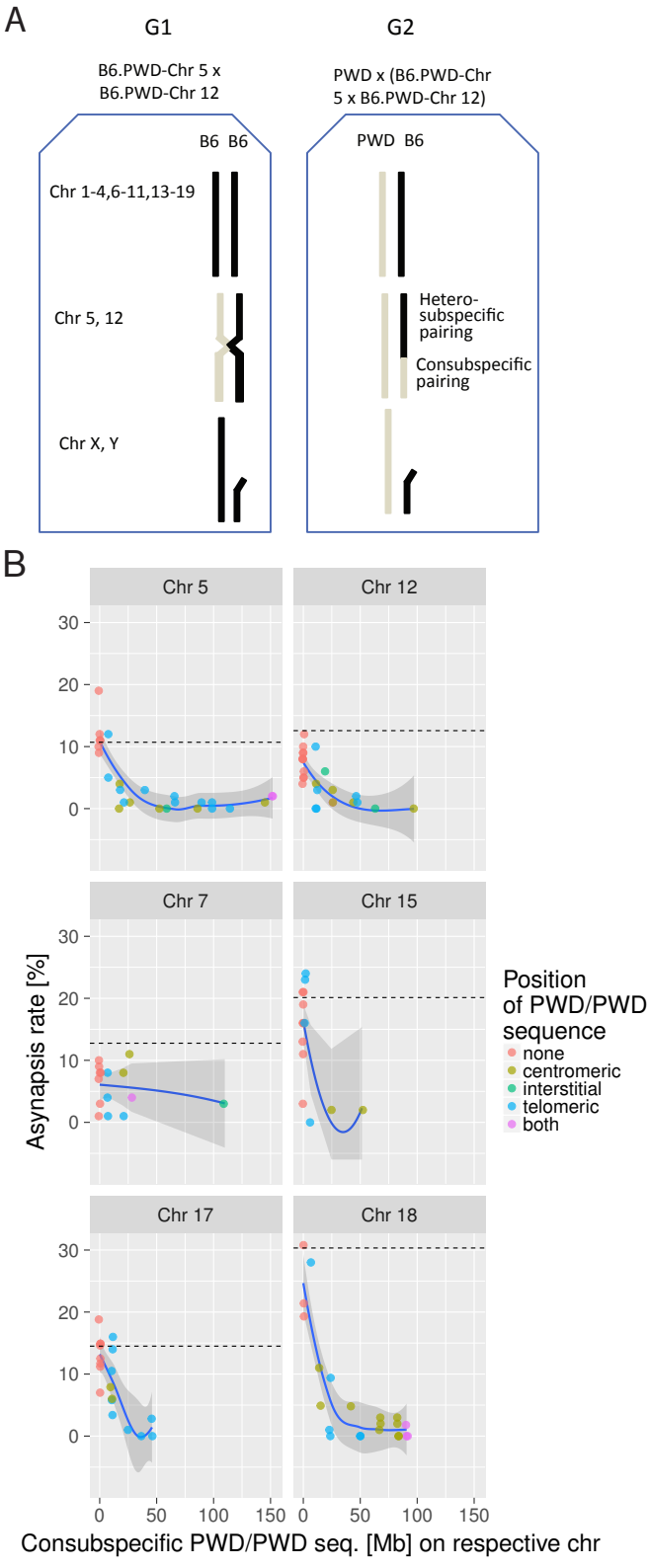
A
G1
G2
B6.PWD-Chr 5 x B6.PWD-Chr 12
PWD x (B6.PWD-Chr 5 x B6.PWD-Chr 12)
B6 B6
PWD B6
Chr 1-4,6-11,13-19
Chr 5, 12
Chr X, Y
Hetero-subspecific pairing
Consubspecific pairing
B
Chr 5
Chr 12
Chr 7
Chr 15
Chr 17
Chr 18
Asynapsis rate [%]
Consubspecific PWD/PWD seq. [Mb] on respective chr
Position of PWD/PWD sequence
none
centromeric
interstitial
telomeric
both

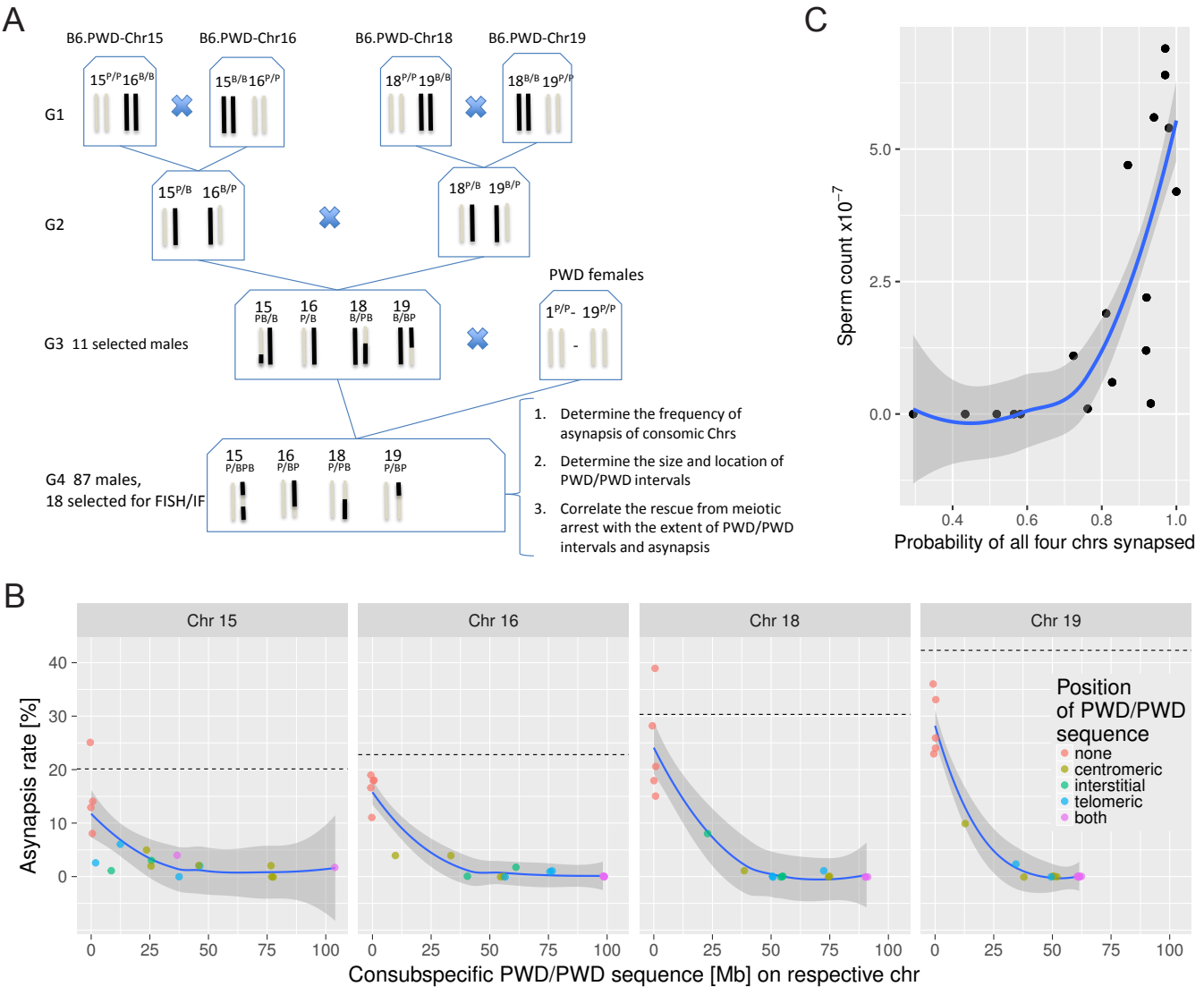
A
B6.PWD-Chr15
B6.PWD-Chr16
B6.PWD-Chr18
B6.PWD-Chr19
G1
G2
G3 11 selected males
G4 87 males,
18 selected for FISH/IF
PWD females
1. Determine the frequency of asynapsis of consomic Chrs
2. Determine the size and location of PWD/PWD intervals
3. Correlate the rescue from meiotic arrest with the extent of PWD/PWD intervals and asynapsis
C
Sperm count x10^-7
Probability of all four chrs synapsed
B
Chr 15
Chr 16
Chr 18
Chr 19
Asynapsis rate [%]
Consubspecific PWD/PWD sequence [Mb] on respective chr
Position of PWD/PWD sequence
none
centromeric
interstitial
telomeric
both

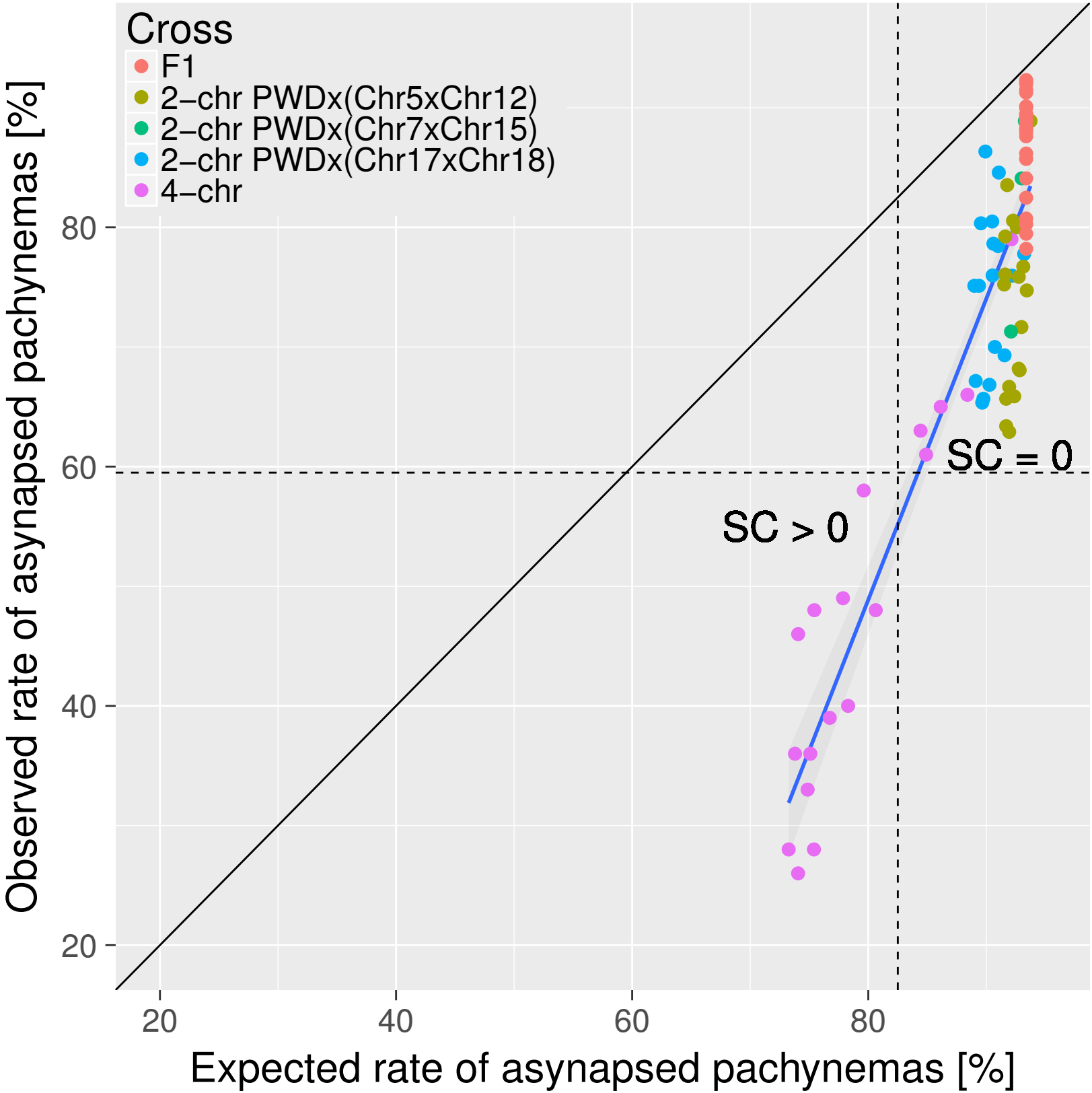
Cross
F1
2−chr PWDx(Chr5xChr12)
2−chr PWDx(Chr7xChr15)
2−chr PWDx(Chr17xChr18)
4−chr
SC = 0
SC > 0
Observed rate of asynapsed pachynemas [%]
Expected rate of asynapsed pachynemas [%]
20
40
60
80
20
40
60
80

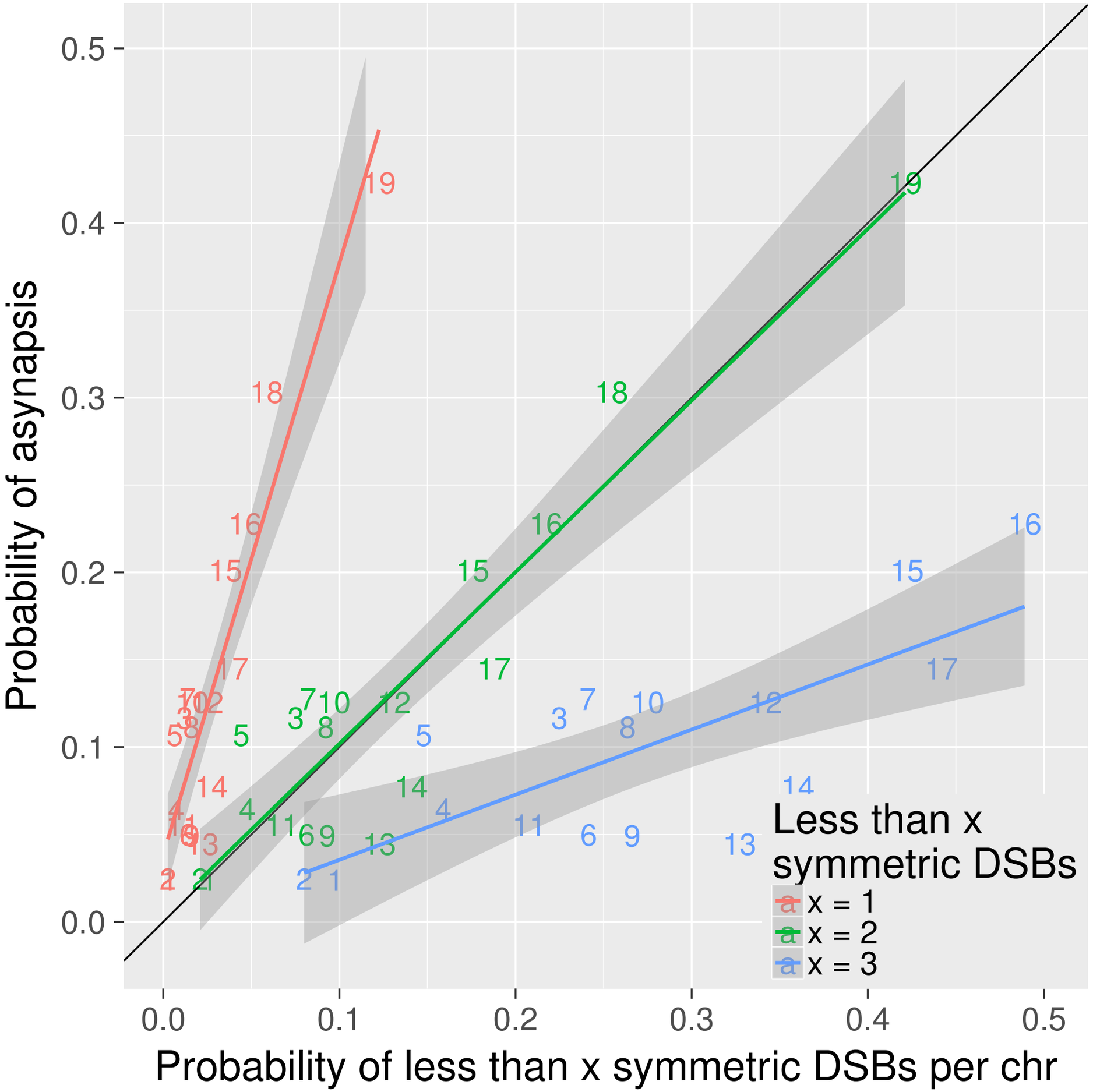
Probability of asynapsis
Probability of less than x symmetric DSBs per chr
0.0
0.1
0.2
0.3
0.4
0.5
Less than x symmetric DSBs
x = 1
x = 2
x = 3